

Tactile-Sensitive NewtonianVAE for High-Accuracy Industrial Connector-Socket Insertion

Ryo Okumura^{*,†}, Nobuki Nishio[†] and Tadahiro Taniguchi^{†,‡}

Abstract— An industrial connector-socket insertion task requires sub-millimeter positioning and compensation of grasp pose of a connector. Thus high accurate estimation of relative pose between socket and connector is a key factor to achieve the task. World models are promising technology for visuo-motor control. They obtain appropriate state representation for control to jointly optimize feature extraction and latent dynamics model. Recent study shows NewtonianVAE, which is a kind of the world models, acquires latent space which is equivalent to mapping from images to physical coordinate. Proportional control can be achieved in the latent space of NewtonianVAE. However, application of NewtonianVAE to high accuracy industrial tasks in physical environments is open problem. Moreover, there is no general frameworks to compensate goal position in the obtained latent space considering the grasp pose. In this work, we apply NewtonianVAE to USB connector insertion with grasp pose variation in the physical environments. We adopt a GelSight type tactile sensor and estimate insertion position compensated by the grasp pose of the connector. Our method trains the latent space in an end-to-end manner, and simple proportional control is available. Therefore, it requires no additional engineering and annotation. Experimental results show that the proposed method, Tactile-Sensitive NewtonianVAE, outperforms naive combination of regression-based grasp pose estimator and coordinate transformation. Moreover, we reveal the original NewtonianVAE does not work in some situation, and demonstrate that domain knowledge induction improves model accuracy. This domain knowledge is easy to be known from specification of robots or measurement.

I. INTRODUCTION

Positioning is one of the fundamental skills in factories, warehouses, retails and so on. It is required in insertion, fitting, pick and place, and other many kinds of industrial operation. Generally, we do not know poses of target objects like holes, sockets, dowel pins and so on. In such cases, we have to localize the target poses from observation, typically images. Recent study shows that robot learning is able to automate those kind of positioning tasks by data driven manner [1]–[4]. The robot learning technology which includes image recognition

^{*} Ryo Okumura and Tadahiro Taniguchi is with Digital & AI Technology Center, Technology Division, Panasonic Corporation, Japan.

[†] Nobuki Nishio is with Innovation Center, Connected Solutions Company, Panasonic Corporation, Japan.

[‡] Tadahiro Taniguchi is also with Ritsumeikan University, College of Information Science and Engineering, Japan.

* Corresponding author: okumura.ryo001@jp.panasonic.com

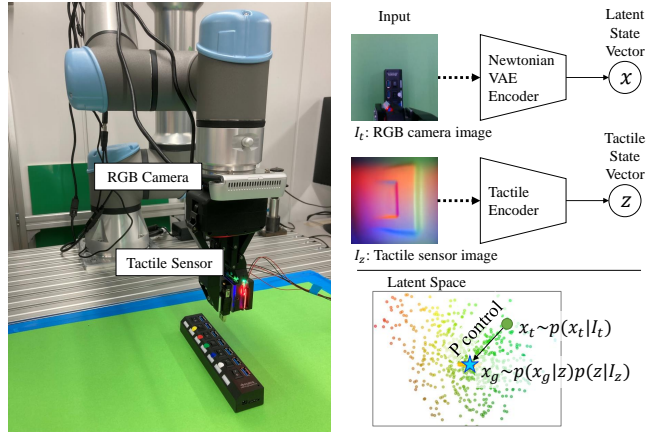


Fig. 1. Overview of proposed robot control system for connector insertion. An underactuated two-finger gripper, RGB camera and GelSight-type tactile sensor are attached to an end of a robot arm. Latent state \mathbf{x} , \mathbf{z} is inferred from an RGB camera images and Tactile sensor image, respectively. A insertion position \mathbf{x}_g is generated from \mathbf{z} . The grasped connector is positioned to the insertion position by proportional control in the latent space, even if there exists grasp pose variations.

is promising because hand-designed feature extraction from the images requires high expertise. It is possible to estimate pose of target objects from the images of external and/or end-effector-attached cameras without the feature engineering by using deep learning based image recognition.

Especially, world models are promising technology for such visuo-motor control. In the world models, appropriate state representation for control is obtained because feature extraction and latent dynamics models are jointly optimized. NewtonianVAE [5], which is a kind of the world models, acquires latent space which is equivalent to mapping from images to physical coordinate. The obtained state representation is appropriate for positioning task. In many positioning tasks, however, not only positioning to target objects, but also compensation for grasp pose variation is problem to be solved. NewtonianVAE does not have mechanism to compensate the grasp pose variation.

Precise estimation of the grasp pose is necessary to solve the problem. Nevertheless, it is hard to estimate the grasp pose from the images of the cameras because the grasped objects are occluded by grippers. GelSight [6] type tactile sensors enable to estimate the grasp pose in sub-millimeter accuracy.

In this paper, we map the end-effector-attached cam-

era images into latent space for positioning the grasped objects, especially USB connectors. The latent space is acquired via NewtonianVAE, to have the same axes as and proportional scale to physical coordinate system. To compensate the grasp pose variation, we adopt the GelSight type tactile sensor. The sensor's raw outputs are directly mapped into insertion position in the latent space, in which the connector is right above a socket. We feedback difference between current and insertion position in the latent space and apply simple proportional control to position the connector just above the socket. The mapping from camera and GelSight image to the latent space is trained in an end-to-end manner.

Our contribution is three-fold.

- We propose a general framework to position the grasped objects to the goal position by visual feedback control via Tactile-Sensitive NewtonianVAE (TS-NVAE). We adopt a GelSight-type tactile sensor to compensate the grasp pose variation in the latent space. TS-NVAE requires no additional feature engineering, annotation nor calibration.
- We demonstrate that the original NewtonianVAE does not work in some situations, and domain knowledge about transition uncertainty and grasp pose variation improves model accuracy. This domain knowledge is easy to be known from specification of robots or measurement.
- We demonstrate that TS-NVAE is applicable for the industrial insertion tasks which requires sub-millimeter positioning accuracy in physical robot control system. TS-NVAE achieves less than 0.5 mm accuracy and outperforms naive combination of regression-based grasp pose estimator and coordinate transformation.

II. RELATED WORK

A. World Models

World model [7] is a generic term used to refer to models that include state inference and transition in partially observable Markov decision process (POMDPs). Joint-optimization of the inference and transition models leads to accurate and sample efficient training. There are roughly three types of control methodology using the trained world models, policy, MPC, and optimal control.

Policy-based method jointly or separately trains policy besides the world models. Lee et. al. [8] has trained the policy by actor-critic method according to theory of control as inference [9]. Hafner et. al. and Okada et. al. [10], [11] have trained the policy from virtually collected transition data in the world models by using overshooting [12] technique. These method require definition of rewards because the policy is optimized to maximize cumulative rewards in an episode. In the connector insertion tasks, it is difficult to measure relative pose between the connectors and sockets, thus dense rewards are generally unavailable. Sparse rewards, however, lead to low sample efficiency. In addition to that, these methods do not work

in an offline learning settings due to difference between learned and behavior policy [13]. Rafael et. al. [14] has alleviated this problem to quantify epistemic uncertainty and induce an uncertainty penalty term into the rewards.

Hafner et. al. and Okada et. al. [12], [15] used MPC [16] in obtained latent space and evaluated performance in MuJoCo [17] simulator environments. MPC infers optimal action sequence by predicting future cumulative rewards, given current states. MPC also needs access to rewards, so the same problem as policy-based method occurs. Moreover, MPC does not work with the sparse rewards in many cases because the future prediction in the latent space do not get any rewards for long time horizon tasks. Extending future prediction horizon needs high computational costs and thus leads to low control frequencies.

Sergey et. al. and Manuel et. al. [1], [18], [19] applied optimal control in the latent space. They induced locally linear constraints into the transition models of the world models. They used off-the-shelf stochastic optimal control methodology like iterative Linear Quadratic Regulator (iLQR) to minimize cost function. The cost function needs to follow a fixed formula, e.g. quadratic function for iLQR. For positioning tasks, square of distance to goal is suitable for the quadratic cost function, but generally we do not have access to the distance in the physical environments.

These existing works above needs access to the rewards, especially distance-based dense rewards, that leads to restrict application to real environments. Therefore, goal conditional control method is preferable for the positioning tasks. Yan et. al. [20] used goal conditional MPC and achieved manipulation of deformable objects. They employed similarity function, distance in the latent space between current and goal states, for objectives of MPC. Angelina et. al. [21] adopted inverse dynamics model to infer action from a pair of sequential observations. They applied constraints by contrastive predictive coding [22] or causal InfoGan [23] to map the sequential observations pair into neighborhood in the latent space.

B. Tactile Sensors

Tactile sensors are important devices for the positioning tasks to estimate the in-hand grasp pose precisely. In this section, we introduce the tactile sensors that have sensing surfaces for contact state perception. [24] developed biomimetic tactile sensors that have multi-modal sensor arrays. [25] utilized MEMS microphone to sense contact forces and paved them under the sensing surface. In the existing works above, however, distance between each sensor element is several millimeters. They do not have sufficient accuracy for the sub-millimeter positioning tasks. Optical tactile sensors [6], [26] utilizes cameras to take images of deformation of the sensing surface. Especially, GelSight is able to measure precise contact shape of the grasped objects. Owing to the high resolution sensor images, GelSight achieved sufficient

accuracy of the grasp pose estimation for connector insertion [27]. They used conventional keypoints matching to localize in-sensor contact pose of the connector, assuming it has no rotation out of sensing surface of the tactile sensor. Then they transformed the in-sensor pose into Cartesian coordinate. For accurate coordinate conversion, relative pose between the robot and the tactile sensor is necessary to be known. They measured it with calibration jig. It is a problem when we want to use underactuated gripper, because relative pose between the robot and gripper changes depending on opening width of the gripper's fingers. Unlike the existing work above, our proposal needs no jig. We do not need to assume that the grasped objects have no rotation out of the sensor surface.

III. PRELIMINARIES

A. NewtonianVAE

NewtonianVAE is one instance of the world models. The highly important feature of NewtonianVAE is that proportional control is possible in the latent space.

NewtonianVAE assumes POMDPs settings where \mathbf{I}_t is observation image, $\mathbf{x}_t \in \mathbb{R}^D$ is latent state and $\mathbf{u}_t \in \mathbb{R}^D$ is action. Note \mathbf{x}_t and \mathbf{u}_t have the same degrees of freedom D to satisfy a formulation discussed below.

They have modeled the transition with double integrator dynamics, inspired by Newton's equations of motion:

$$\begin{aligned}\frac{d\mathbf{x}}{dt} &= \mathbf{v} \\ \frac{d\mathbf{v}}{dt} &= A(\mathbf{x}, \mathbf{v}) \cdot \mathbf{x} + B(\mathbf{x}, \mathbf{v}) \cdot \mathbf{v} + C(\mathbf{x}, \mathbf{v}) \cdot \mathbf{u}\end{aligned}$$

They trained the world models to maximize the lower bound below:

$$\begin{aligned}\mathcal{L} &= \mathbb{E}_{q(\mathbf{x}_t|\mathbf{I}_t)q(\mathbf{x}_{t-1}|\mathbf{I}_{t-1})} [\mathbb{E}_{p(\mathbf{x}_{t+1}|\mathbf{x}_t, \mathbf{u}_t; \mathbf{v}_t)} p(\mathbf{I}_{t+1}|\mathbf{x}_{t+1}) \\ &+ \text{KL}(q(\mathbf{x}_{t+1}|\mathbf{I}_{t+1})\|p(\mathbf{x}_{t+1}|\mathbf{x}_t, \mathbf{u}_t; \mathbf{v}_t))]\end{aligned}\quad (1)$$

where the transition prior is:

$$p(\mathbf{x}_t|\mathbf{x}_{t-1}, \mathbf{u}_{t-1}; \mathbf{v}_t) = \mathcal{N}(\mathbf{x}_t|\mathbf{x}_{t-1} + \Delta t \cdot \mathbf{v}_t, \sigma^2) \quad (2)$$

$$\mathbf{v}_t = \mathbf{v}_{t-1} + \Delta t \cdot (A\mathbf{x}_{t-1} + B\mathbf{v}_{t-1} + C\mathbf{u}_{t-1}) \quad (3)$$

with

$$\begin{aligned}A &= \text{diag}(f_A(\mathbf{x}_t, \mathbf{v}_t, \mathbf{u}_t)) \\ \log(-B) &= \text{diag}(f_B(\mathbf{x}_t, \mathbf{v}_t, \mathbf{u}_t)) \\ \log C &= \text{diag}(f_C(\mathbf{x}_t, \mathbf{v}_t, \mathbf{u}_t))\end{aligned}$$

where f_A, f_B, f_C is a neural network with linear output activation. \mathbf{v}_t is computed as $\mathbf{v}_t = (\mathbf{x}_t - \mathbf{x}_{t-1})/\Delta t$. Because transition matrices A, B, C are diagonal, linear combinations between each latent dimension is eliminated. Therefore, correct coordinate relations between \mathbf{u} , \mathbf{x} and \mathbf{v} are obtained.

For a physical robot experiment, they set $A = 0$, $B = 0$, $C = 1$ to improve sample efficiency. They also added an additional regularization term to the latent space, $\text{KL}(q(\mathbf{x}|\mathbf{I})\|\mathcal{N}(0, 1))$.

Proportional control like Mixture Density Network [28] and Dynamic Movement Primitives [29], [30] have been performed in the acquired latent space.

B. GelSight

GelSight is an optical tactile sensor. It composes of a color camera, RGB colors of LEDs, clear gel whose one side surface is covered with opaque thin coating. The LEDs' light is emitted to the coating through the gel. The camera captures images of the coating illuminated by the LEDs through the gel. If objects contact the other side of surface of the coating, the gel and coating deform. Thus, the camera captures deformation of contact surface. The obtained images are used for 3D reconstruction [6]. Tian et. al. utilize the RGB images directly to control robots [31]. In this paper, we use the RGB images directly like Tian et. al. to estimate the insertion pose.

IV. TACTILE-SENSITIVE NEWTONIANVAE

A. Training Objective

Our work is built upon NewtonianVAE. We jointly train a goal state prediction model from the tactile sensor images besides the NewtonianVAE latent model, given:

- image-action sequences $D_x = (\mathbf{I}_1, \mathbf{u}_1), \dots, (\mathbf{I}_T, \mathbf{u}_T)$
- a pair of images $D_z = (\mathbf{I}_z, \mathbf{I}_g)$

where \mathbf{I}_t is a camera image, \mathbf{I}_z is a tactile sensor image and \mathbf{I}_g is a camera image at the insertion position. Our training objective is $\mathcal{L}_x + \mathcal{L}_z$ such that:

$$\begin{aligned}\mathcal{L}_x &= \mathbb{E}_{q(\mathbf{x}_t|\mathbf{I}_t)} \mathbb{E}_{p(\mathbf{x}_{t+1}|\mathbf{x}_t, \mathbf{u}_t)} [-p(\mathbf{I}_{t+1}|\mathbf{x}_{t+1}) \\ &+ \text{KL}(q(\mathbf{x}_{t+1}|\mathbf{I}_{t+1})\|p(\mathbf{x}_{t+1}|\mathbf{x}_t, \mathbf{u}_t))]\end{aligned}\quad (4)$$

$$\begin{aligned}\mathcal{L}_z &= \mathbb{E}_{q(\mathbf{z}|\mathbf{I}_z)q(\mathbf{x}_g|\mathbf{I}_g)} \mathbb{E}_{p(\mathbf{x}_g|\mathbf{z})} [-p(\mathbf{I}_z|\mathbf{z}) \\ &- p(\mathbf{I}_g|\mathbf{x}_g) + \text{KL}(q(\mathbf{x}_g|\mathbf{I}_g)\|p(\mathbf{x}_g|\mathbf{z}))]\end{aligned}\quad (5)$$

We employed built-in Cartesian velocity control function of the robot, i.e. \mathbf{u}_t is reference velocity in Cartesian space. We simplify the transition prior of NewtonianVAE as below:

$$p(\mathbf{x}_t|\mathbf{x}_{t-1}, \mathbf{u}_{t-1}) = \mathcal{N}(\mathbf{x}_t|\mathbf{x}_{t-1} + \Delta t \cdot \mathbf{u}_t, \sigma_x^2) \quad (6)$$

Owing to the simplified prior, the latent space has the same axes and scales as the Cartesian coordinate system.

B. Induce domain knowledge

Assuming the latent and Cartesian space have the same axes and scales, we can easily induce domain knowledge into the latent distribution. First, σ_x in the prior represents transition uncertainty of the robots. We set $\sigma_x = 0.0001$, that is nominal repeated positioning accuracy of the UR5e (0.1 mm). Moreover, we further add additional KL terms to the training objective.

$$\begin{aligned}\mathbb{E}_{q(\mathbf{z}|\mathbf{I}_z)q(\mathbf{x}_g|\mathbf{I}_g)} \mathbb{E}_{p(\mathbf{x}_g|\mathbf{z})} [\text{KL}(q(\mathbf{x}_g|\mathbf{I}_g)\|\mathcal{N}(0, \sigma_g^2)) \\ + \text{KL}(p(\mathbf{x}_g|\mathbf{z})\|\mathcal{N}(0, \sigma_g^2))]\end{aligned}\quad (7)$$

σ_g represents variation of insertion position. In the context of our problem settings, it is equivalent to the

grasp pose variation. In our experiments described below σ_g is set to 0.0015 because the grasp pose variation is $\pm 2\sigma_g = 0.003$ mm.

V. EXPERIMENT

A. Hardware Configuration

Fig. 1 shows our experimental setup. A robot arm is a 6-DoF Universal Robots UR5e robot. An end-effector is a ROBOTIS RH-P12-RN(A) underactuated two-finger gripper. An Intel RealSense camera has been attached to a tool mount of the UR5e. In our experiment, depth images are not used. We have attached a GelSight-type tactile sensor to one finger of the gripper. A target USB socket has been attached to a table. The sockets have seven holes. We have used only center one of them. We have used only the camera and tactile images for control, so the controller does not have access to Cartesian nor joint pose of the robot arm. We have used the built-in Cartesian velocity control in X and Y axes in the UR5e.

B. Data collection

Fig. 2 shows a graphical model and our data collection process. The robot pulls out the USB connector from the socket, and observe the first camera image \mathbf{I}_0 and tactile image \mathbf{I}_z . In this time, the robot should be at insertion position corresponding to the grasp pose variation that is able to be observed by \mathbf{I}_z and represented by z . Thus, \mathbf{I}_0 is treated as \mathbf{I}_g during training. Then the robot randomly walks above the socket and collect transition data tuple $(\mathbf{I}_t, \mathbf{u}_t)$. The random action was sampled uniformly from -0.01 to 0.01 m/s. This data collection process provides assurance that the insertion position \mathbf{x}_g exists in episodes, that leads to train positional relationship between the insertion position \mathbf{x}_g and other position \mathbf{x}_t via the transition prior Eq. (6). We collected 30 trajectories for experiments. One episode has 10 seconds length, and control frequency is 2 Hz, i.e. one episode has 20 transitions. So we totally collected only 300 seconds, 600 transitions for training.

C. Training

We have used 224×224 and 64×64 RGB images as inputs of camera and tactile encoders, respectively. ResNet [32] with 18 layers has been employed for a camera image encoder. The camera encoder is pre-trained on ImageNet [33]. The output of the last layer of the encoder is then fed into fully connected layer to infer the posterior. We have used simple CNN for a tactile image encoder. Since the tactile images have large domain shift from ImageNet or other large-scale open datasets, we did not use pre-trained model for the tactile encoder. We have adopted fully connected networks with 2 hidden layers with 16 units and LeakyReLU activation to infer \mathbf{x}_t, \mathbf{z} from encoded features. Insertion position estimator $p(\mathbf{x}_g|\mathbf{z})$ is also fully connected neural network that has the same structure as the inference model of \mathbf{x}_t and \mathbf{z} . All posterior and prior have been modeled as Gaussian

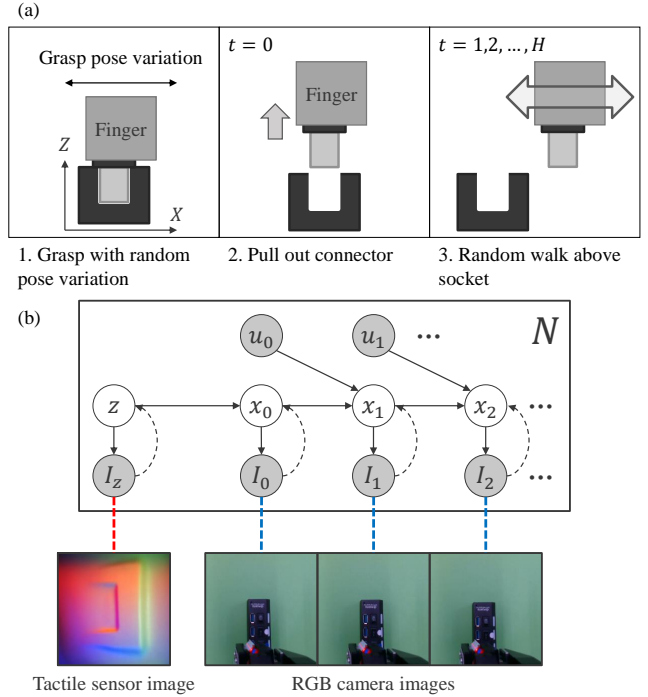


Fig. 2. (a) Data collection process. First, a robot grasps a connector with a random pose. Second, it pulls out the connector upward. In this time, we observe \mathbf{I}_z and \mathbf{I}_0 . \mathbf{I}_0 is treated as \mathbf{I}_g during training of insertion position estimator $p(\mathbf{x}_g|\mathbf{z})$. Then the robot randomly walks above a socket to collect transition data. Time horizon H is 20, episode number N is 30. (b) Graphical model. \mathbf{x}_0 is a latent state at the insertion pose, and generated from \mathbf{z} .

distribution. We have inputted 8 full sequences for one-step backpropagation, and executed totally 100k steps of training (About 50k epochs). All models were trained using Adam [34] with a learning rate of 3×10^{-4} .

D. Experiment 1. Visualization

After training, we have visualized acquired latent space. We compare our proposal to some instances of NewtonianVAE (Fig. 3). We also perform ablation study. Validation dataset for this experiment contains 70 new episodes collected with the same procedure as the training data. For NewtonianVAE baselines, action is acceleration. We added the action to current velocity to make reference velocity to control the UR5e robot arm by velocity control. Upper row of Fig. 3 shows latent maps. Variation of marker color hue and saturation represents X, Y position of the Cartesian coordinate, respectively. Blue star represents estimated insertion positions from the tactile images. Second and third row show correlation between the X, Y position and corresponding latent state, respectively. The latent state of our proposed method, TS-NVAE, shows high correlation to physical coordinate system. Insertion position estimation is accurate. NVAE is naive NewtonianVAE whose transition matrices are $A = 0$, $B = 0$, $C = 1$. In NVAE/trainABC, the transition matrices are trainable. In NVAE+tactile, a training objective includes \mathcal{L}_z in Eq. 5. For three NewtonianVAE baselines,

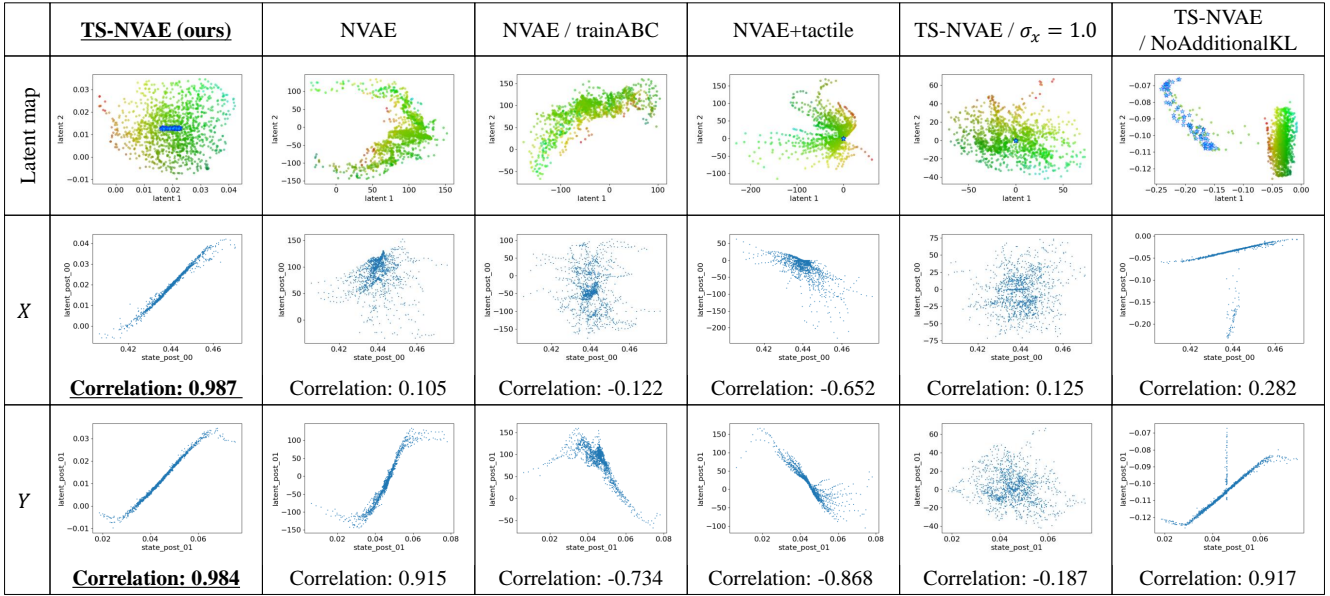


Fig. 3. Visualization of latent spaces. Upper row shows latent maps whose horizontal and vertical axis is the first and second dimension of latent states. Marker color represents position in Cartesian coordinate system. Color variation from red to green represents X position in the Cartesian coordinate system. Color saturation represents Y, high saturation means high Y position. Blue stars represent estimated insertion positions from tactile images. In NVAE and NVAE/trainABC, insertion positions are not plotted because tactile-sensor-related models are not trained. Second and third row represents correlation between X, Y position in the Cartesian coordinate and corresponding latent state, respectively. TS-NVAE is our proposal. NVAE means naive NewtonianVAE whose transition matrices are $A = 0$, $B = 0$, $C = 1$. In NVAE/trainABC, the transition matrices are trainable. In NVAE+tactile, a training objective includes \mathcal{L}_z . TS-NVAE/ $\sigma_x=1$ and TS-NVAE/NoAdditionalKL are ablation study. In TS-NVAE/ $\sigma_x=1$, we do not use domain knowledge about transition uncertainty and set $\sigma_x = 1.0$. In TS-NVAE/NoAdditionalKL, we do not use additional KL term in Eq. 7 for training.

the correlation between physical and latent position is low. Because the domain knowledge about transition uncertainty is not used, σ_x is set to 1.0 that is too large value for this system. In NVAE+tactile, insertion position estimation from the tactile images fails because latent space does not reflect transition model of NewtonianVAE. TS-NVAE/ $\sigma_x=1$ and TS-NVAE/NoAdditionalKL are ablation study. In TS-NVAE/ $\sigma_x=1$, we do not use domain knowledge about transition uncertainty and set $\sigma_x = 1.0$. This value is dissociated from true transition uncertainty, thus correlation to physical coordinate is low. In TS-NVAE/NoAdditionalKL, we do not use additional KL term in Eq. 7 for training. Without the additional KL term, insertion position is not mapped correctly into the latent space. Correlation is high except for the insertion position.

TABLE I
PERFORMANCE FOR CONNECTOR INSERTION TASK

	Success Rate	Accuracy [mm]
TS-NVAE	40/40	0.29 ± 0.14
NVAE	0/10	82.75 ± 41.54
NVAE/trainABC	0/10	130.94 ± 8.52
NVAE+tactile	0/10	123.38 ± 43.32
TS-NVAE/NoAdditionalKL	0/10	126.07 ± 13.00
TS-NVAE/ $\sigma_x=1$	0/10	125.24 ± 14.40
Regression	36/40	No data

E. Experiment 2. Positioning performance

We have evaluated positioning accuracy by using simple proportional control in the latent space. Velocity reference is \mathbf{u}_t calculated $\mathbf{u}_t = \alpha(\mathbf{x}_g - \mathbf{x}_t)$. α is set to 1, and control frequency is 20 Hz. Table I shows success rate of the connector insertion and mean/standard of positioning. Our method achieved higher success rate and positioning accuracy than other method.

VI. CONCLUSION

We have proposed a general framework to position the grasped connector to the insertion position by visual feedback control considering the grasp pose variation without any additional feature engineering, annotation nor calibration. Domain knowledge about transition uncertainty and grasp pose variation has been induced as fixed standard deviation of Gaussian distribution. This domain knowledge is easy to be known from specification of robots or measurement. Model accuracy has been improved by the domain knowledge induction. Our proposed framework achieves higher performance compared to the naive combination of regression-based grasp pose estimator and coordinate transformation in the connector-insertion task in the physical environment.

VII. FUTURE WORK

We can extend our method to full-pose proportional control. In general, the conventional localization technique like template matching can not estimate angles

accurately. Therefore, data driven method is more important in the full-pose control. Adaptation to contact-rich environments is also interesting direction. To feed-back contact force measure by the tactile sensors, force-sensitive latent dynamics and proportional control can be achieved. The current control system is disrupted if the target objects are framing out, or occluded by other objects. Introducing recurrent architecture to use observation history is able to be a valid measure against the problem.

REFERENCES

- [1] S. Levine, N. Wagener, and P. Abbeel, “Learning contact-rich manipulation skills with guided policy search,” in *ICRA*, 2015.
- [2] G. Schoettler, A. Nair, J. Luo, S. Bahl, J. Ojea, E. Solowjow, and S. Levine, “Deep reinforcement learning for industrial insertion tasks with visual inputs and natural rewards,” in *IROS*, 2020.
- [3] T. K. Lars Berscheid, Pascal Meißner, “Self-supervised learning for precise pick-and-place without object model,” in *RA-L*, 2020.
- [4] E. Johns, “Coarse-to-fine imitation learning: Robot manipulation from a single demonstration,” *2021 IEEE International Conference on Robotics and Automation (ICRA)*, pp. 4613–4619, 2021.
- [5] M. Jaques, M. Burke, and T. M. Hospedales, “NewtonianVAE: Proportional control and goal identification from pixels via physical latent spaces,” in *Proceedings of the IEEE/CVF Conference on Computer Vision and Pattern Recognition (CVPR)*, pp. 4454–4463, June 2021.
- [6] M. Johnson and E. Adelson, “Retrographic sensing for the measurement of surface texture and shape,” in *CVPR*, pp. 1070–1077, 06 2009.
- [7] D. Ha and J. Schmidhuber, “Recurrent world models facilitate policy evolution,” in *NIPS*, 2018.
- [8] A. X. Lee, A. Nagabandi, P. Abbeel, and S. Levine, “Stochastic latent actor-critic: Deep reinforcement learning with a latent variable model,” in *arXiv*, 2019.
- [9] S. Levine, “Reinforcement learning and control as probabilistic inference: Tutorial and review,” *ArXiv*, vol. abs/1805.00909, 2018.
- [10] D. Hafner, T. Lillicrap, J. Ba, and M. Norouzi, “Dream to control: Learning behaviors by latent imagination,” in *ICLR*, 2020.
- [11] M. Okada and T. Taniguchi, “Dreaming: Model-based reinforcement learning by latent imagination without reconstruction,” *2021 IEEE International Conference on Robotics and Automation (ICRA)*, pp. 4209–4215, 2021.
- [12] D. Hafner, T. Lillicrap, I. Fischer, R. Villegas, D. Ha, H. Lee, and J. Davidson, “Learning latent dynamics for planning from pixels,” in *ICML*, 2019.
- [13] A. Kumar, A. Zhou, G. Tucker, and S. Levine, “Conservative q-learning for offline reinforcement learning,” in *ICML*, 06 2020.
- [14] R. Rafailov, T. Yu, A. Rajeswaran, and C. Finn, “Offline reinforcement learning from images with latent space models,” in *Learning for Dynamics and Control*, pp. 1154–1168, PMLR, 2021.
- [15] M. Okada, N. Kosaka, and T. Taniguchi, “Planet of the bayesians: Reconsidering and improving deep planning network by incorporating bayesian inference,” *arXiv*, 2020.
- [16] C. E. Garcia, D. M. Prett, and M. Morari, “Model predictive control: Theory and practice - a survey,” in *Automatica*, 1989.
- [17] E. Todorov, T. Erez, and Y. Tassa, “Mujoco: A physics engine for model-based control,” in *IROS*, 2012.
- [18] S. Levine and P. Abbeel, “Learning neural network policies with guided policy search under unknown dynamics,” *Advances in neural information processing systems*, vol. 27, 2014.
- [19] M. Watter, J. Springenberg, J. Boedecker, and M. Riedmiller, “Embed to control: A locally linear latent dynamics model for control from raw images,” *Advances in neural information processing systems*, vol. 28, 2015.
- [20] W. Yan, A. Vangipuram, P. Abbeel, and L. Pinto, “Learning predictive representations for deformable objects using contrastive estimation,” *arXiv preprint arXiv:2003.05436*, 2020.
- [21] A. Wang, T. Kurutach, K. Liu, P. Abbeel, and A. Tamar, “Learning robotic manipulation through visual planning and acting,” *arXiv preprint arXiv:1905.04411*, 2019.
- [22] A. Van den Oord, Y. Li, and O. Vinyals, “Representation learning with contrastive predictive coding,” *arXiv e-prints*, pp. arXiv-1807, 2018.
- [23] A. Wang, T. Kurutach, K. Liu, P. Abbeel, and A. Tamar, “Learning robotic manipulation through visual planning and acting,” in *RSS*, 2019.
- [24] N. Wettels, J. A. Fishel, Z. Su, C. H. Lin, G. E. Loeb, and L. SynTouch, “Multi-modal synergistic tactile sensing,” in *Tactile sensing in humanoids—Tactile sensors and beyond workshop, 9th IEEE-RAS international conference on humanoid robots*, 2009.
- [25] B. Lammers, “Design and realisation of a haptic interface between a reflex takktile and an omega 7 haptic device,” B.S. thesis, University of Twente, 2017.
- [26] K. Kamiyama, H. Kajimoto, K. Vlack, N. Kawakami, T. Mizota, and S. Tachi, “Gelforce,” in *ACM SIGGRAPH 2004 Emerging technologies*, p. 5, 2004.
- [27] R. Li, R. Platt, W. Yuan, A. ten Pas, N. Roscup, M. A. Srinivasan, and E. Adelson, “Localization and manipulation of small parts using gelsight tactile sensing,” in *2014 IEEE/RSJ International Conference on Intelligent Robots and Systems*, pp. 3988–3993, IEEE, 2014.
- [28] C. M. Bishop, “Mixture density networks,” in *Technical Report NC RG/94/004*, Aston University, 1994.
- [29] A. J. Ijspeert, J. Nakanishi, H. Hoffmann, P. Pastor, and S. Schaal, “Dynamical movement primitives: learning attractor models for motor behaviors,” *Neural computation*, vol. 25, no. 2, pp. 328–373, 2013.
- [30] S. Schaal, “Dynamic movement primitives-a framework for motor control in humans and humanoid robotics,” in *Adaptive motion of animals and machines*, pp. 261–280, Springer, 2006.
- [31] S. Tian, F. Ebert, D. Jayaraman, M. Mudigonda, C. Finn, R. Calandra, and S. Levine, “Manipulation by feel: Touch-based control with deep predictive models,” *2019 International Conference on Robotics and Automation (ICRA)*, pp. 818–824, 2019.
- [32] K. He, X. Zhang, S. Ren, and J. Sun, “Deep residual learning for image recognition,” in *2016 IEEE Conference on Computer Vision and Pattern Recognition (CVPR)*, (Los Alamitos, CA, USA), pp. 770–778, IEEE Computer Society, jun 2016.
- [33] J. Deng, W. Dong, R. Socher, L.-J. Li, K. Li, and L. Fei-Fei, “Imagenet: A large-scale hierarchical image database,” in *2009 IEEE conference on computer vision and pattern recognition*, pp. 248–255, Ieee, 2009.
- [34] D. Kingma and J. Ba, “Adam: A method for stochastic optimization,” *International Conference on Learning Representations*, 12 2014.